THE RASSF8 CANDIDATE TUMOUR SUPPRESSOR INHIBITS CELL GROWTH AND REGULATES THE WNT AND NF-KB SIGNALLING PATHWAYS VIA ADHERENS JUNCTIONS.

Frances E. Lock, Thomas Dunwell, Luke Hesson, David Gomez, Wendy Cooper, Nicholas Underhill-Day, Asha Recino, Andrew Ward, Tatiana Pavlova, Eugene Zabarovsky, Melissa M. Grant, Eamonn R Maher, Andrew Chalmers, Walter Kolch, Farida Latif.

ABSTRACT

The Ras-assocation domain family (RASSF) of tumor suppressor proteins until recently contained six proteins named *RASSF1–6*. Recently, four novel family members, RASSF7–10, have been identified by homology searches for RA-domain-containing proteins. These additional RASSF members are divergent and structurally distinct from *RASSF1–6*, containing an N-terminal RA domain and lacking the Sav/RASSF/Hpo (SARAH) domain. Here, we show that *RASSF8* is ubiquitously expressed throughout the murine embryo and in normal human adult tissues. Functionally, RNAi-mediated knockdown of RASSF8 in non-small-cell lung cancer (NSCLC) cell lines, increased anchorage-independent growth in soft agar and enhanced tumor growth in severe combined immunodeficiency (SCID) mice. Furthermore, EdU staining of RASSF8-depleted cells showed growth suppression in a manner dependent on contact inhibition. We show that endogenous RASSF8 is not only found in the nucleus, but is also membrane associated at sites of cell–cell adhesion, co-localizing with the adherens junction (AJ) component β-catenin and binding to E-cadherin. Following RASSF8 depletion in two different lung cancer cell lines using alternative small interfering RNA (siRNA) sequences, we show that AJs are destabilized and E-cadherin is lost from the cell membrane. The AJ components β-catenin and p65 are also lost from sites of cell–cell contact and are relocalized to the nucleus with a concomitant increase in β-catenin-dependent and nuclear factor-κB (NF-κB)-dependent signaling following RASSF8 depletion. RASSF8 may also be required to maintain actin -cytoskeletal organization since immunofluorescence analysis shows a striking disorganization of the actin- cytoskeleton following RASSF8 depletion. Accordingly, scratch wound healing studies show increased cellular migration in RASSF8-deficient cells. These results implicate *RASSF8* as a tumor suppressor gene that is essential for maintaining AJs function in epithelial cells and have a role in epithelial cell migration.

INTRODUCTION

The classical Ras-association domain family (RASSF1-6) are a group of Ras-effector molecules that contain a C-terminal Ras-association (RA) domain of the Ra1GDS/AF-6 variety and a protein interaction domain known as the Sav/RASSF/Hippo (SARAH) domain (Scheel and Hofmann, 2003). Several members of the RASSF family are involved in tumorigenesis as epigenetic inactivation of many isoforms is a frequent event across many tumor types (Hesson *et al.*, 2007a). Several RASSF members show functions consistent with roles as tumor suppressor proteins such as the regulation of apoptosis through interactions with pro-apoptotic proteins such as the mammalian Ser/Thr kinases 1 and 2 (MST1/2) and modulator of apoptosis 1 (MOAP-1), which are known to interact with residues within the Sav/RASSF/Hippo (SARAH) domain (Hesson *et al.*, 2007b; Richter *et al.*, 2009). In addition, RASSF1A has a

major role in the regulation of microtubule dynamics during mitotic progression and loss of RASSF1A results in RAN GTPase-dependent progression delay through pro-metaphase leading to genomic instability and aneuploidy (Vos *et al.*, 2004; Dallol*et al.*, 2004, 2009). RASSF1A depletion has also been shown to result in reduced cell–cell adhesion and changes in morphology (Dallol *et al.*, 2005).

Recently, several additional RA-domain-containing family members have been identified and designated as N-terminal RASSF proteins (RASSF7–10) (Sherwood*et al.*, 2008). These comprise RASSF7 (also known as HRC1), RASSF8 (also known as HOJ-1 or C12ORF2), RASSF9 (also known as P-CIP1 or PAMCI) and RASSF10. These proteins are divergent and structurally distinct from RASSF1–6, contain an RA domain within their extreme N-termini and lack the Sav/RASSF/Hpo (SARAH) protein interaction domain. RASSF7–10 represent an evolutionarily conserved group of proteins with orthologs of all four in the lower vertebrate*Xenopus laevis* and a RASSF7/8 homolog in *Drosophila melanogaster* distinct from the RASSF1–6 *Drosophila* homologs. Little is known about the N-terminal RASSF7–10 proteins. Recently we have shown that *Xenopus* RASSF7 is a centrosome-associated protein and is required for completing mitosis (Sherwood*et al.*, 2008). There is some evidence suggesting that RASSF8 may act as a tumor suppressor gene in lung cancer (Falvella *et al.*, 2006). RASSF9 has been shown to bind RAS proteins and is linked to vesicle trafficking (Chen *et al.*, 1998;Rodriguez-Viciana *et al.*, 2004). Finally, RASSF10 is frequently and epigenetically inactivated in leukemia (Hesson *et al.*, 2009). In this report, we provide evidence that RASSF8 is a lung cancer tumor suppressor gene that regulates cell–cell adhesion and actin cytoskeleton organization by having a critical role in maintaining AJ stability.

RESULTS

RASSF8 is ubiquitously expressed
In order to characterize *RASSF8*, we assessed *RASSF8* expression in mouse embryos. *RASSF8* mRNA expression was assessed by *in situ* hybridization in normal E15.5 mice embryos by using RASSF8 antisense probes. RASSF8 mRNA expression was observed in the major organs, including brain, heart, kidney, liver, lung and spinal cord (Figure 1a). We also performed expression analysis on a range of adult normal human tissues. Using primers that amplify across exons 4–6, we found that the *RASSF8* gene is expressed in all tissues analyzed, including the lung (Supplementary Figure S1A). These studies illustrate the ubiquitous expression pattern of RASSF8 throughout murine embryos and normal human adult tissues, but very little is currently known about the role and function of RASSF8 in these tissues.
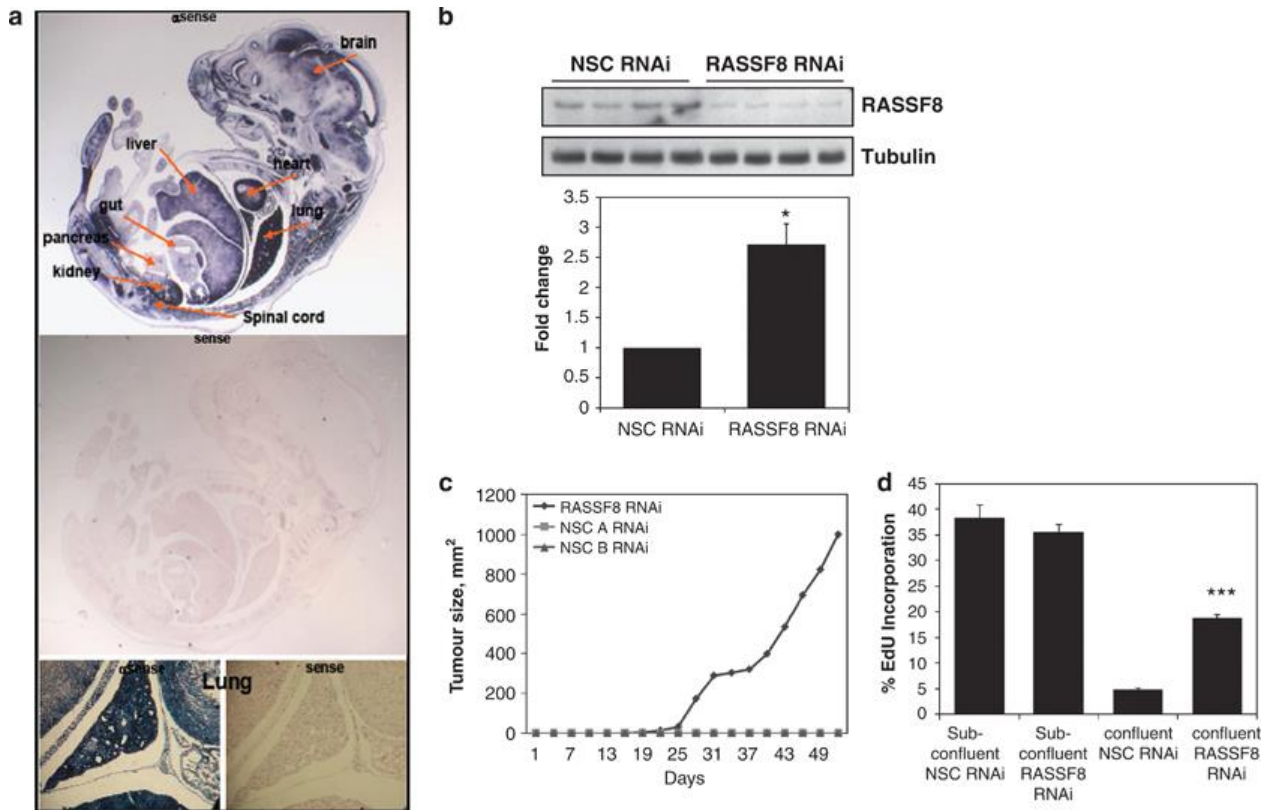
FIGURE 1

RASSF8 mRNA expression and tumor suppression. (A) In situ hybridization to assess RASSF8 RNA expression and localisation in E15.5 embryonic mouse demonstrated Rassf8 mRNA expression in several major organs, including the lung. (B) A549-RASSF8-RNAi, and A549-NSC cell lysates were subjected to Western blotting to analyse RASSF8 expression. RASSF8 expression is knocked down in A549-RASSF8-RNAi lysates compared to NSC controls. Tubulin expression was also assessed as a loading control. (C) A549 RNAi cells were cultured in soft agar for 5 weeks to assess anchorage independent cell growth. The total number of colonies over 100µm across were counted. This experiment was repeated on three separate occasions, mean and SEM are shown as fold change compared to A549 NSC-RNAi cells. * P=<0.05. (D) Tumourigenicity of A549-RASSF8-RNAi and A549-NSC-RNAi control cells was assayed by subcutaneous injection into SCID mice. Animals were maintained according to institutional guidelines. (E) % EdU incorporation for sub-confluent and confluent A549 cells with RASSF8 RNAi or control (NSC) knockdown cells. In confluent cells RASSF8 RNAi vs NSC RNAi, *** P=<0.001. No difference was seen in sub-confluent cells.

RASSF8 suppresses tumor cell growth

To observe the effects of loss of *RASSF8* expression, A549 lung carcinoma cells were stably transfected with GFP-IRES-shRNAmir constructs specifically targeting RASSF8 or a non-silencing control non-silencing control (NSC) to generate A549-RASSF8-RNAi and A549-NSC (non-silencing control) cells, respectively. Depletion of RASSF8 protein was verified by western blotting using an antibody directed against RASSF8 (Figure 1b, top panel). Cells with RASSF8 depletion showed a 2.7-fold increase in anchorage-independent growth in soft agar when compared with A549 cells expressing RNAi NSC sequence (Figure 1b, bottom panel). Transient depletion of RASSF8 using alternative siRNA sequences also resulted in a threefold increase in anchorage-independent growth of the lung cancer cell line H1792 (Supplementary Figures S1B and C).

RASSF8 depletion promotes *in vivo* tumorigenicity in severe combined immunodeficiency (SCID) mice

A549-RASSF8-RNAi and A549-NSC cells were also inoculated into SCID mice to study tumor growth *in vivo*. RNAi stable cells were mixed with matrigel and inoculated into three mice. Solid tumor nodes were only formed at the inoculation point and their size was measured with calipers. Over the course of 52

days, solid tumors were detected for all the mice inoculated with the A549-RASSF8-RNAi cells but no tumors were observed for mice inoculated with A549-NSC cells (Figure 1c). Thus, we have shown that *RASSF8* may function as a tumor suppressor gene *in vitro* and more importantly *in vivo.* In the above experiments, 10^4 cells were inoculated into SCID mice and we did not see tumor formation in control mice. In other experiments, when we inoculated 10^7 or 10^6 cells we observed tumors in control mice. In fact if we could have kept the mice for longer than 52 days we would get tumors also in controls even with a lower number of cells. But because of the institutional guidelines for the SCID mouse experiments, we had to stop the procedure at 52 days.

RASSF8-depleted cells increase EdU incorporation in confluent cells

Preliminary growth curve data suggested that RASSF8-depleted cells continued to proliferate even after cells reach confluency whereas control cells did not, suggesting a reduction in contact-dependent growth inhibition. Hence, we examined EdU incorporation as an index of DNA synthesis in dividing cells. In A549 confluent cells, RASSF8-depleted cells showed significantly more EdU incorporation compared with control cells ($P<0.001$), while in subconfluent cells no differences were seen in percentage EdU incorporation between RASSF8-depleted and control cells ($P=0.39$) (Figure 1d). Thus, RASSF8-depleted cells continue to divide rapidly post-confluency, indicating further loss of contact-dependent inhibition.

RASSF8 knockdown in *Xenopus* results in enhanced cell proliferation

To further determine the role of RASSF8 in cell proliferation *in vivo,* we performed morpholino-mediated knockdown studies in *X. laevis* embryos. MO2 directed against *RASSF8* substantially downregulated RASSF8 protein, MO1 also downregulated RASSF8 protein but to a much lesser extent then MO2, while control morpholinos had no effect on RASSF8 protein level (Supplementary Figure S1D, left panel). We counted the number of cells stained for phospho-histone H3 (a marker for cell proliferation) in each section. We noticed a significant increase in cell proliferation in RASSF8-depleted cells (MO2) compared with control cells ($P=0.0465$) (Supplementary Figure S1D, middle and right panels). Whereas MO1 proliferation increased slightly, this was not significant. Hence, the differences in cell proliferation directly reflect the amount of RASSF8 protein present. These data add further evidence to the role of RASSF8 in controlling cell proliferation.

RASSF8 localizes to AJs

In order to examine the cellular localization of endogenous RASSF8, parental A549 and H1792 lung cancer cells were immunostained and examined by confocal microscopy. In A549 parental cells, endogenous RASSF8 was observed within the nucleus and at the cell membrane specifically at sites of cell–cell contact (Figure 2a and Supplementary Figures S2A and B). In both A549 and H1792 parental cells RASSF8 immunostaining co-localized with the AJ component β-catenin (Figure 2a and Supplementary Figure S3A).
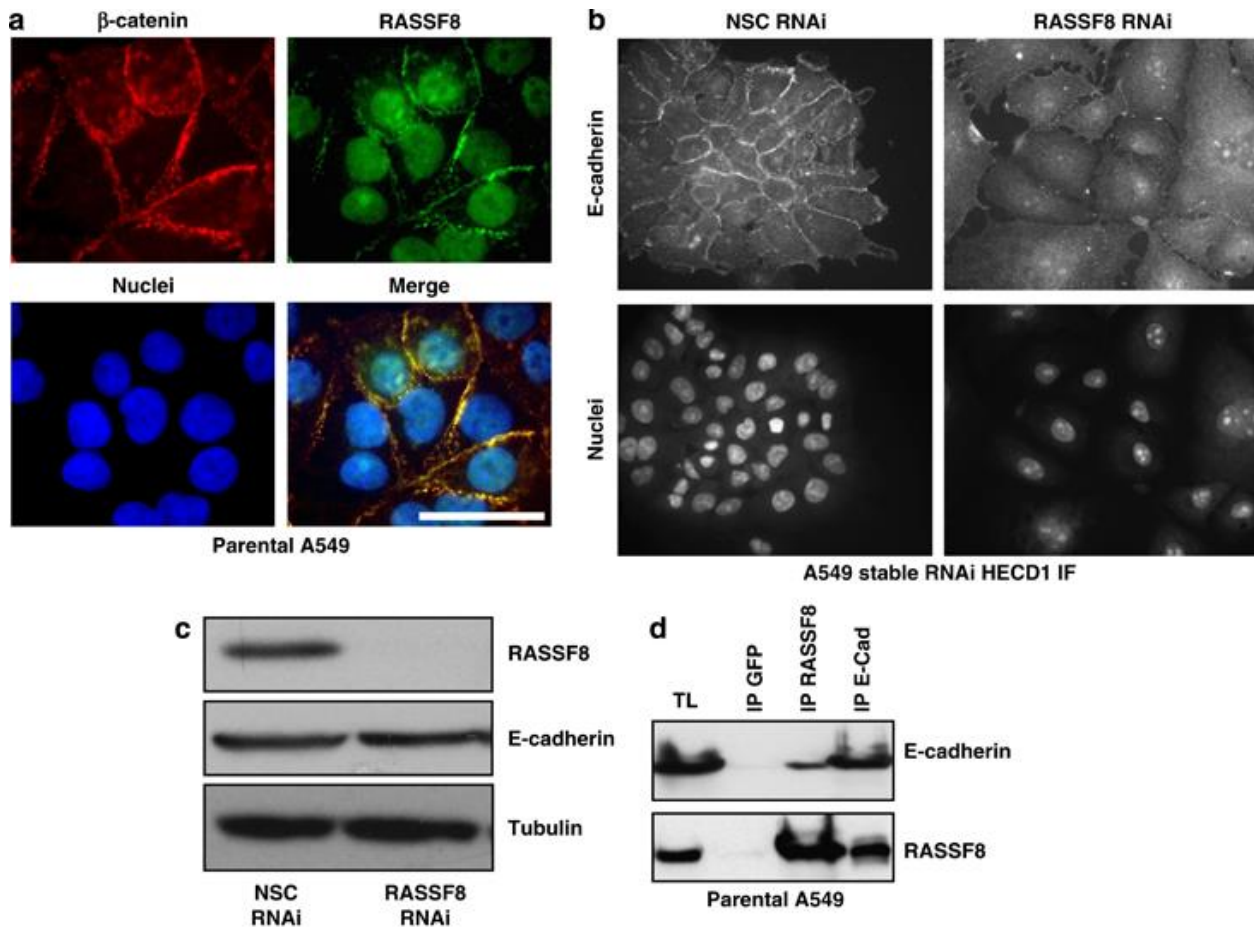
FIGURE 2

Endogenous RASSF8 cellular localization. (A) In order to analyse endogenous RASSF8 localization, parental A549 cells were fixed, stained with RASSF8 and β-catenin antibodies and a nuclear stain, then subjected to confocal microscopy. Endogenous RASSF8 is found in the nucleus and cytoplasm, but is also localised to cell-cell junctions, where it colocalises with β-catenin at adherens junctions. (B) A549-RNAi cells were subjected to epifluorescence immunostaining for E-cadherin. A549-NSC cells grow in well organised colonies, with E-cadherin localised to cell-cell junctions. Following RASSF8 depletion, E-cadherin is lost from cell junctions and cells grow in a more dispersed manner. Insert scale bars!! (C) A549-RASSF8-RNAi, and A549-NSC cell lysates were subjected to Western blotting. No significant changes in E-caderin expression were observed. Tubulin expression was also assessed as a loading control. Blot is representative of 4 separate experiments. (D) A549-RNAi cells were subjected to confocol immunostaining for β-catenin. In A549-NSC cells β–catenin is localized to adherens junctions at the cell periphery. Following RASSF8 depletion, β–catenin is lost from cell junctions and is relocalized to nuclear and peri-nuclear regions in the cell. (E) A549-RASSF8-RNAi, and A549-NSC cell lysates were subjected to Western blotting. No significant changes in β-catenin expression were observed. Tubulin expression was also assessed as a loading control. Blot is representative of 4 separate experiments. (F) The activity of a β-catenin/TCF-dependent promoter (TOP) was determined in A549 RNAi cells by luciferase assay. A549 RNAi cells were transiently transfected with 1 μg TOPFlash (TCF/LEF activity reporter construct) and 0.1 μg of pRL-TK (Renilla luciferase transfection control), cultured for 24h, lysed, and luciferase activity was analyzed. Data shown are the mean and SEM from three separate experiments, expressed as fold change compared to A549-NSC-RNAi cells. P=<0.01. Scale bar represents 10μ meter in all immunofluorescence images.

RASSF8 depletion inhibits AJs formation

Adherens junctions are located at the points of contact between cells and are indispensible to both epithelial cell polarity and normal tissue architecture. AJs maintain cell–cell adhesion mediated through homotype interactions between E-cadherin molecules on neighboring cells. E-cadherin homodimers span the plasma membrane to interact with β-catenin, which binds E-cadherin cytoplasmic tails and

forms a part of a complex consisting of α-catenin and p120 catenin that links E-cadherin to actin filaments. Disruption of AJs is thought to result in reduced cell–cell adhesion and to permit the increased motility of normal cells or the invasion and metastasis of cancer cells.

Given the localization of human RASSF8 at AJs, we hypothesized that RASSF8 may be involved in maintaining AJ formation and stability. Using immunofluorescence, we analyzed the subcellular distribution of E-cadherin in A549-RASSF8-RNAi and control cells. In A549-NSC cells, E-cadherin is localized to the cell periphery at cell–cell contacts. Following RASSF8 depletion, cells are more spread out, with E-cadherin staining relocalized from cell–cell contacts to diffuse staining of the cytoplasm (Figure 2b). Loss of tight, intercellular contact is clearly observed. Western blotting analysis confirmed that the total levels of E-cadherin remain unchanged following RASSF8 depletion in A549 cells (Figure 2c). Transient depletion of RASSF8 using alternative siRNA sequences in another lung cancer cell line, H1792, gave similar results (Supplementary Figures S3B and C).

Endogenous RASSF8 interacts with endogenous E-cadherin
We investigated whether RASSF8 and E-cadherin directly interact in mammalian cells. Endogenous E-cadherin and RASSF8 were immunoprecipitated using specific antibodies against these proteins in parental A549 cells. As shown in Figure 2d, we could detect the presence of E-cadherin in RASSF8 immunoprecipitates. The interaction between E-cadherin and RASSF8 was also observed when we used E-cadherin antibody to immunoprecipitate the complex (Figure 2d). This confirmed E-cadherin and RASSF8 do indeed interact at the endogenous level in mammalian cells.

β-Catenin and the canonical Wnt signaling pathway
β-Catenin has two distinct functions. When located at the cell periphery, β-catenin is a major cytoplasmic component of AJs. However, β-catenin is also found in a cytoplasmic pool and can enter the nucleus to mediate the Wnt signaling pathway. The canonical Wnt/β-catenin pathway has a key role in embryogenesis and also in the malignant transformation of cells. The oncogenic properties of this pathway stem from the relocalisation of β-catenin at the cell membrane to the nucleus, where it binds the T-cell factor/lymphoid enhancer factor (TCF-LEF) family of transcription factors to form a bipartite transcription factor, which facilitates the transcription of target genes. These target genes encode effector proteins that promote proliferation, invasion and inhibit apoptosis. In this way, regulation of β-catenin subcellular localization is an important mechanism in regulating the canonical Wnt/β-catenin pathway.

As shown earlier, RASSF8 co-localizes with β-catenin at the cell periphery in parental A549 and H1792 lung cancer cells (Figure 2a and Supplementary Figure S3A). The subcellular distribution of β-catenin was determined by confocal immunofluorescence in A549 RNAi cells. In NSC cells, β-catenin is localized to the cell periphery and involved in AJs. Following RASSF8 depletion, β-catenin is relocalised from cell–cell contacts and accumulates in the cytoplasm and nucleus (Figure 3a). The same experiment was repeated following transient siRNA depletion of RASSF8 in H1792 cells (using alternative siRNA sequences), which confirmed this observation (Supplementary Figure S3C). Western blotting analysis confirmed that the total levels of β-catenin remain constant following RASSF8 depletion (Figure 3b and Supplementary Figure S3B).
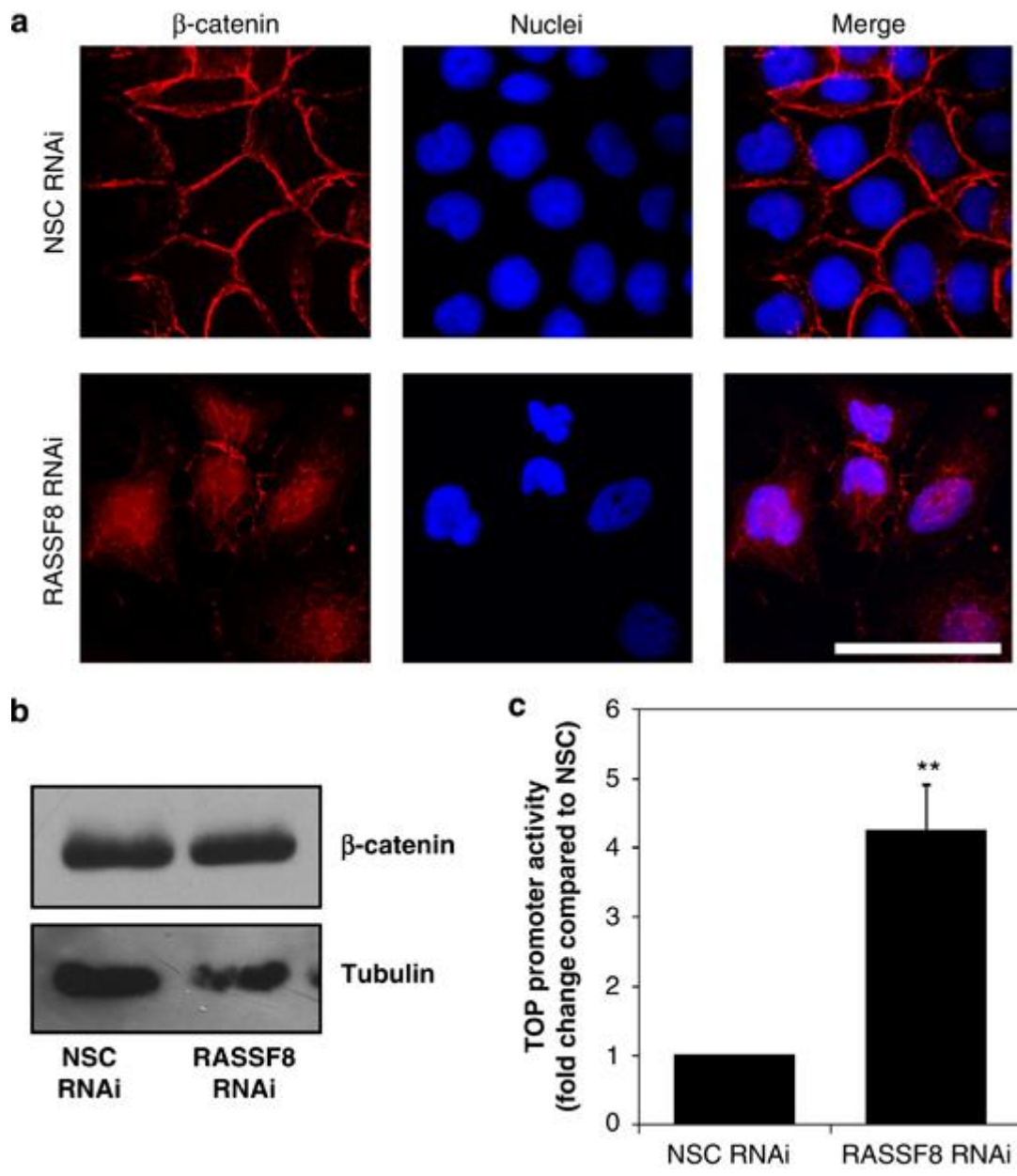
FIGURE 3

RASSF8 depletion results in p65 relocalization. (A) A549 parental cells were fixed, stained using β-catenin and p65 antibodies and examined by confocal microscopy. p65 is localized to the cell periphery, co-localising with β–catenin at adherens junctions. (B) A549-RNAi cells were subjected to confocal immunostaining for p65. In A549-NSC cells p65 is localized to adherens junctions at the cell periphery. Following RASSF8 depletion, p65 is lost from cell junctions and is relocalized to nuclear and peri-nuclear regions in the cell. (C) The activity of a NF-κB-dependent promoter was determined in A549 RNAi cells by luciferase assay. A549 RNAi cells were transiently transfected with 1 μg 3nehGL4.2 (p65 -dependent promoter activity reporter construct) and 0.1 μg of pRL-TK (Renilla Luciferase transfection control), cultured for 24h, lysed, and luciferase activity was analyzed. A small but significant 1.6 fold increase in p65-dependent promoter activity was observed following FASSF8 knockdown. Data shown are the mean and SEM from three separate experiments, expressed as fold change compared to A549-NSC-RNAi cells. P=<0.01 (D) A549-RNAi cellular levels of the p65 regulator IκB-α were analysed by immunoblotting. Following RASSF8 knockdown, IkB- α levels were significantly decreased compared to NSC control cell lysates. Tubulin expression was also assessed as a loading control. This experiment was repeated on three separate occasions, with a representative blot shown. Scale bar represents 10μ meter in all immunofluorescence images.

In the nucleus, β-catenin can interact with the T-cell factor/lymphoid enhanced factor (TCF-LEF) family of transcription factors to facilitate the activation of target genes as part of the canonical Wnt signaling pathway. The activity of a β-catenin/TCF-dependent promoter (TOP) was determined in A549 RNAi cells. A significant increase in β-catenin/TCF-dependent promoter (TOP)-dependent promoter activity was observed following RASSF8 knockdown (Figure 3c;$P<0.01$). Again, this result was confirmed following transient RASSF8 depletion in H1792 cells (Supplementary Figure S3D; $P<0.001$).

p65 localization at AJs is abolished following RASSF8 depletion

The NF-κB family of transcription regulators is ubiquitously expressed in most eukaryotic cells and is found in the cytoplasm as homo- or heterodimers. Nuclear factor-κB (NF-κB) transcription factors are implicated in carcinogenesis and cellular transformation (Downward, 2009). All family members share a REL-homology domain (RHD), which is required for nuclear localization, DNA binding and interaction with the IκB regulatory proteins. The most well-characterized member of this family is NF-κB p65. It has been reported that the p65 subunit of the NF-κB heterodimer associates with β-catenin and other components of AJs (Deng *et al.*, 2002; Solanas *et al.*, 2008). Indeed, β-catenin may also regulate the NF-κB signaling pathway in some cell types (Deng *et al.*, 2004). We also observed p65 localized to AJs, co-localizing with β-catenin in parental A549 lung cancer cells (Figure 4a) and in H1792 cells (Supplementary Figure S4A).
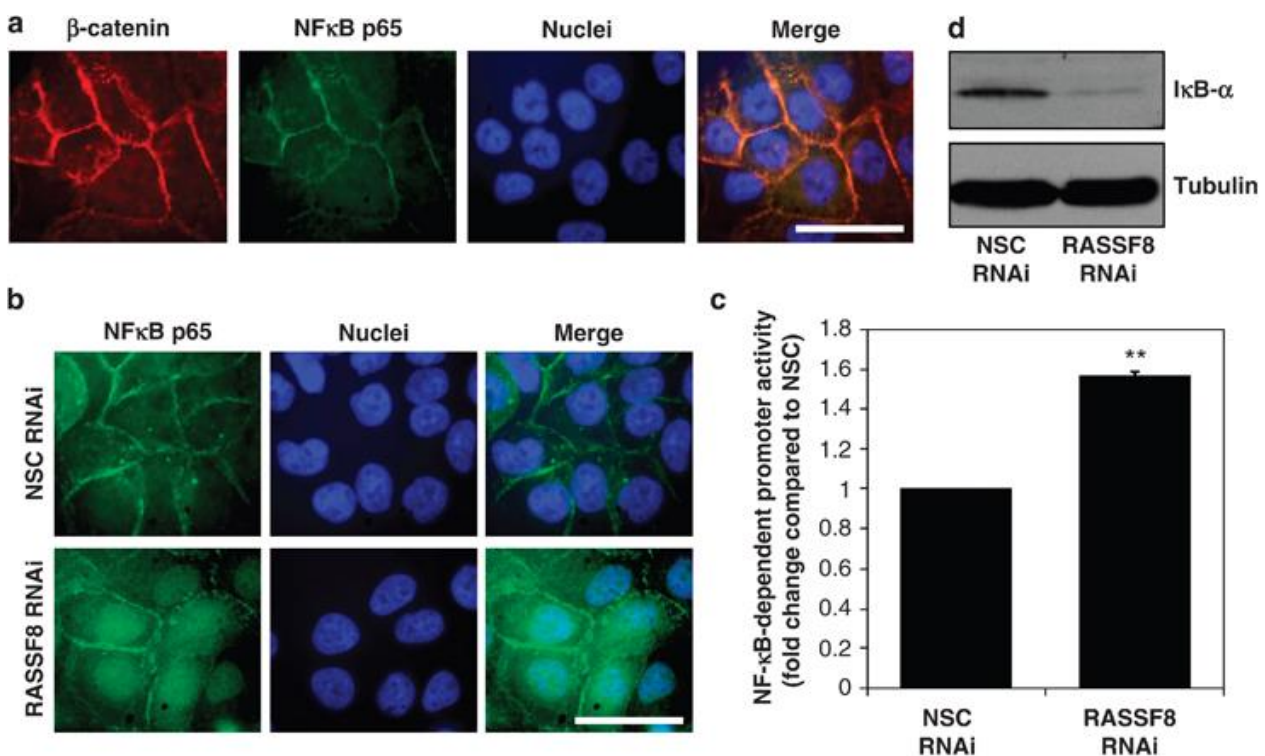
Figure 4.

FIGURE 4

RASSF8 depletion results in p65 relocalization. (**a**) A549 parental cells were fixed, stained using β-catenin and p65 antibodies and examined by confocal microscopy. p65 is localized to the cell periphery, co-localizing with β-catenin at adherens junctions (AJs). (**b**) A549-RNAi cells were subjected to confocal immunostaining for p65. In A549-NSC cells p65 is localized to AJs at the cell periphery. Following RASSF8 depletion, p65 is lost from cell junctions and is relocalized to nuclear and perinuclear regions in the cell. (**c**) The activity of a NF-κB-dependent promoter was determined in A549 RNAi cells by luciferase assay. A549 RNAi cells

Previous work has shown that disruption of functional AJs can lead to relocation of p65 from the cell periphery to the nucleus, where it can promote NF-κB-dependent transcription of target genes that encode pro-mitotic and anti-apoptotic proteins (Deng _et al._, 2002). Therefore, the importance of RASSF8 expression in regulating the subcellular distribution of p65 was determined by confocal immunofluorescence in A549 RNAi cells. In parental and NSC cells, p65 is localized to the cell periphery and co-localizes with β-catenin at AJs (Figures 4a and b). Following RASSF8 depletion, p65 is relocalized from cell–cell contacts and accumulates in the cytoplasm and nucleus (Figure 4b). Nuclear p65 increased >2.5-fold in RASSF8-depleted A549 cells (Supplementary Figure S5). The same experiment was repeated following transient siRNA depletion of RASSF8 in H1792 cells, which confirmed this observation (Supplementary Figure S4B).

NF-κB promoter-dependent signaling is increased following RASSF8 knockdown
The activity of an NF-κB-dependent promoter was determined in A549 RNAi and control cells. A significant increase in NF-κB-dependent promoter activity was observed following RASSF8 knockdown (Figure 4c; $P<0.01$). This experiment was repeated using RASSF8 transient depletion in H1792, where RASSF8 knockdown again induced an increase in NF-κB-dependent promoter activity (Supplementary Figure S4C; $P<0.05$).

p65 binds to target DNA sequences called κB sites found on the promoter and enhancer regions of target genes. At these sites, p65 can interact with a co-adapter and bridging proteins to transactivate a variety of genes (including c-myc, p53 and some cyclins) involved in cell cycle control to promote cellular transformation and inhibit apoptosis. In unstimulated cells, inactive NF-κB–p65 dimeric complexes are bound to its regulatory protein IκB-α. Signal transduction leading to NF-κB–p65 activation is processed through IκB-α as IκB-α binding masks the nuclear localizing signal of NF-κB–p65 dimers. Cell stimulation leading to IκB-α dissociation from p65 also results in phosphorylation of IκB-α, targeting IκB-α for degradation by the 26S proteosome, and allowing p65 dimers to enter the nucleus (Hayden and Ghosh, 2008).

IκB-α cellular levels in A549 cells were analyzed by western blotting. Following RASSF8-RNAi, IκB-α levels were significantly depleted, compared with NSC-RNAi controls (Figure 4d). This result was also observed in H1792 cells following transient depletion of RASSF8 (Supplementary Figure S4D). Hence, RASSF8 depletion results in NF-κB activation in lung cancer cells.

RASSF8 is required for cytoskeleton organization
The observed changes in AJ formation and cell morphology following RASSF8 depletion led us to look at the morphology of the actin cytoskeleton in these cells. A549-RNAi cells were fixed and stained with alexa-phalloidin to visualize the actin cytoskeleton. A549-NSC cells have an organized actin cytoskeleton, with actin bundles and stress fibers clearly visible. Following RASSF8 depletion, the actin cytoskeletal architecture appears very disorganized, with few stress fibers seen (Figure 5a). A similar change in actin cytoskeleton morphology was also observed in H1792 transiently transfected with RASSF8 siRNA (Supplementary Figure S6).
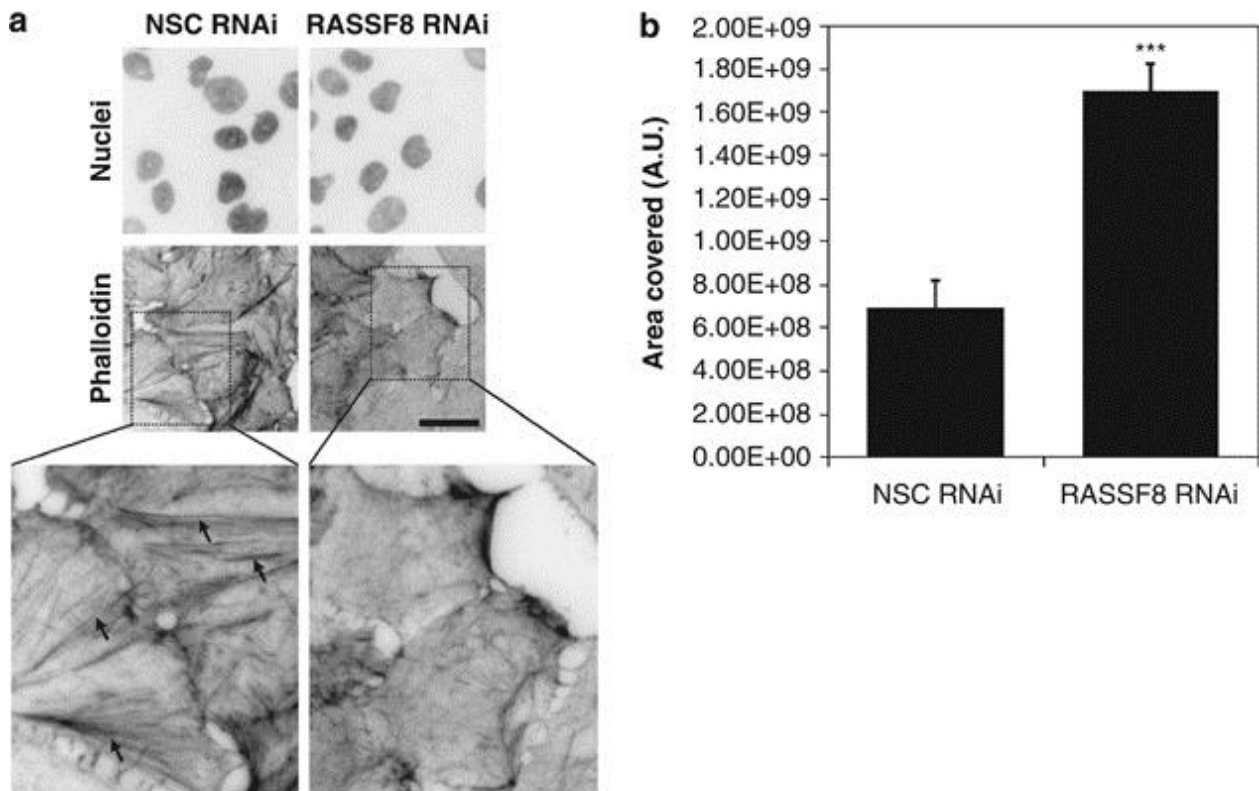
FIGURE 5

RASSF8 role in cell migration. (**a**) A549-RNAi cells were subjected to epifluorescence immunostaining with alexa-phalloidin to visualize the actin cytoskeleton. Images were inverted for clarity. A549-NSC cells have an organized actin cytoskeleton, with actin bundles and stress fibers clearly visible (black arrows). Following RASSF8 depletion, the actin cytoskeleton appears disorganized, with few stress fibers seen. (**b**) RASSF8 role in migration was assessed by scratch wound healing assay. Confluent monolayers of mitotically inactivated A549-NSC and A549-RASSF8 RNAi cells were scratched with a pipette tip and the resulting migration into the 'wound' was assessed. RASSF8 depletion resulted in significantly increased migration compared to NSC-RNAi control cells. ***P<0.001.

Having observed a significant change in actin morphology, we also assessed the *in vitro* migration ability of A549-RNAi cells using a scratch wound-healing assay. Seven hours after wounding, the area of the wound covered was assessed. A549-RASSF8-RNAi cells covered a significantly greater wound area, compared with the A549-NSC cells, suggesting that cell migration and motility are significantly increased following RASSF8 knockdown (Figure 5b and Supplementary Figure S7;*P*<0.001).

DISCUSSION

RASSF8 is a novel tumor suppressor *in vivo* and *in vitro*
RASSF8 represents an intriguing new member of the RASSF family. Here, we confirmed that RASSF8 mRNA is expressed in all the major organs and tissues, including the lung, during murine embryonic development and in normal adult human tissues. Closer examination by confocal immunofluorescence studies also revealed that RASSF8 is found in the nucleus and also concentrated at the cell membrane at the AJs in lung cancer cells.

It has been recently suggested that *RASSF8* may be a novel tumor suppressor gene in lung cancer (Falvella *et al.*, 2006). Overexpression of this isoform suppresses anchorage-independent growth of the lung cancer cell lines A549 and H520 (Falvella *et al.*, 2006). As overexpression can often lead to toxicity, we aimed to investigate the effects of decreased levels of RASSF8 (as observed in lung cancer) on cell growth by RNAi-mediated RASSF8 depletion. Both transient and stable depletion of RASSF8 in H1792 and A549 lung cancer cells, respectively, resulted in accelerated anchorage-independent growth in soft agar providing further evidence that physiological levels of RASSF8 suppress cell growth. RASSF8-depleted A549 cells injected into SCID mice also resulted in increased tumor formation compared with mice injected with control cells, showing, for the first time, that physiological levels of RASSF8 are required to suppress tumor growth *in vivo*. Increase in cell proliferation was also seen in *Xenopus* embryos with RASSF8 depletion compared with control cells, providing further evidence for the role of RASSF8 acting as a tumor suppressor gene.

Proliferation studies of control A549 and RASSF8-depleted stable cells suggested similar rates of proliferation up to the point of confluency, after which RASSF8-depleted A549 cells continued to proliferate. Indeed, we show that RASSF8-depleted cells increase EdU incorporation in confluent cells but not in subconfluent cells. This suggests that RASSF8 suppresses growth in a manner dependent on contact inhibition, a physiological process whereby the proliferation of normal cells is limited by their physical contact with neighboring cells.

RASSF8 expression is required for AJ stability

Endogenous RASSF8 localizes to AJs in lung cancer cells and binds to E-cadherin. Following RASSF8 depletion, E-cadherin total expression levels remain unchanged. However, E-cadherin localization is lost from the discrete localization at the cell membrane to diffuse staining within the cytoplasm. This observation was confirmed by confocal microscopy analysis of β-catenin staining. Following RASSF8 depletion, β-catenin is lost from AJs and accumulates in the cytoplasm and nucleus. This suggests that the AJ formation and function is lost following RASSF8 depletion. Lack of stabilization of β-catenin at AJs allows β-catenin relocalization to the nucleus, where it can promote activation of the canonical Wnt signaling pathway by interacting with the T-cell factor/lymphoid enhanced factor (TCF-LEF) family of transcription factors and facilitating the activation of TCF-dependent genes (Brembeck *et al.*, 2006; MacDonald *et al.*, 2009). We observed a significant increase in β-catenin/TCF-dependent promoter activity following RASSF8 depletion. Together, these data suggest that RASSF8 depletion may result in increased β-catenin/TCF signaling, as part of the canonical Wnt signaling pathway.

It has been previously shown that disruption of functional AJs can lead to relocation of p65 from the cell periphery to the nucleus, where it can promote NF-κB-dependent transcription of target genes. Following RASSF8 depletion, we also observed a relocalization of p65 from AJs to the perinuclear and nuclear regions of the cell. Promoter activity analysis confirmed a significant increase in NF-κB-dependent promoter activity following RASSF8 knockdown.

p65 signaling requires the regulatory protein IκB-α to be phosphorylated and degraded, allowing p65 dimers to enter the nucleus and activate target genes. Western blotting confirmed that IκB-α cellular levels were significantly depleted following RASSF8 depletion. Together, these data suggest that the NF-κB p65 signaling pathway is upregulated following RASSF8 depletion. The observed decrease in the level of IκB-α correlates with increased nuclear NF-κB and is likely a result of its phosphorylation by the multisubunit IkappaB kinase (IKK). The effect on RASSF8 knockdown on the mechanics of IκB-α regulation/degradation presents opportunities for future study.

Together, these findings suggest that RASSF8 expression may control cellular proliferation of non-small cell lung cancer (NSCLC) cells by regulating β-catenin localization and the canonical Wnt signaling pathway and, concomitantly, p65 localization and the NF-κB signaling pathway.

RASSF8 may have a role in actin cytoskeleton organization and cell motility
In lung carcinoma cells, the actin cytoskeleton is organized into stress fibers, which span the cell cytoplasm, linking to the catenins in AJs to anchor at the cell membrane. The observed disruption of AJs following RASSF8 depletion is the likely cause of the observed disruption and disorganization of the actin cytoskeleton in these cells. We also observed a significant increase in cell motility following RASSF8 knockdown in A549 cells, which may be a functional consequence of the observed disorganization of the actin cytoskeleton. These data suggest that loss of RASSF8 expression may have an important role in stabilizing the actin cytoskeleton and thus repressing cell migration. RASSF8 has also been implicated in a familial form of synpolydactyly (Debeer *et al.*, 2002). A reciprocal chromosomal translocation t(12;22)(p11.2;q13.3) involving *RASSF8* and the Fibulin-1 (*FBLN1*) gene was identified in three patients from one family sharing a complex type of synpolydactyly. It is at present unclear what role disruption of RASSF8 may have in the observed limb malformations. However, it is intriguing to speculate that the role of RASSF8 in regulating cell–cell adhesion may contribute to the development of normal tissue architecture.

A role for RASSF family members in controlling cell adhesion is not without precedence. An isoform of RASSF5 (also known as RAPL) regulates the redistribution of lymphocyte-function-associated antigen 1 (LFA-1) at the cell membrane to enhance adhesion to intercellular adhesion molecule 1 (ICAM-1) T-cell immunological synapses (Katagiri *et al.*, 2003). Furthermore, we previously showed that RASSF1A depletion results in changes in cell morphology, increased cellular migration and reduced cell–cell adhesion (Dallol *et al.*, 2005). These examples provide evidence that several members of the RASSF family are important adaptor proteins in signaling pathways that link the cytoskeletal framework of cells to cell membrane receptor complexes.

RASSF7 is the RASSF protein with the most sequence similarity to RASSF8. However, our results suggest that there are significant differences between the functions of RASSF7 and RASSF8. We show that RASSF8 localizes to sights of cell–cell contact and in the nucleus. In contrast RASSF7 localizes to the centrosome (Sherwood *et al.*, 2008). Knocking down RASSF7 in *Xenopus* embryos produced a striking increase in nuclear fragmentation (Sherwood *et al.*, 2008); when we knocked down RASSF8 we did not see this fragmentation. In contrast, knocking down RASSF8 produced an increase in proliferation, something that was not seen after knocking down RASSF7 (Sherwood *et al.*, 2008). This suggests that the two genes have diverged in their function. In *Drosophila,* there is one gene that is related to RASSF7 and RASSF8, and it appears that the function of this gene is more similar to RASSF8 than RASSF7 (Langton *et al.*, 2009). Langton *et al.* have recently described the role of *Drosophila* dASPP-dRASSF8 in regulating cell–cell adhesion during *Drosophila* retinal morphogenesis.

AJs are essential for maintaining tissue architecture. They are also involved in the maintenance of tissue homeostasis, promote cell-to-cell communication, increase resistance to apoptosis, regulate cell shape and polarity (Dejana and Rudini, 2008). In this report, we have provided evidence that RASSF8 loss leads to enhanced cell proliferation *in vivo* and loss of AJ function, thereby deregulating the Wnt and NF-κB signaling pathways in cancer. Hence, a member of the N-terminal RASSF family may be essential for maintaining AJ function in epithelial cells.

Supplementary data

Detailed experimental procedures and additional figures are provided in supplementary section.

ACKNOWLEDGEMENTS

MATERIALS AND METHODS

Cell culture

Cell culture medium and reagents were purchased from Invitrogen. A549 and H1792 were maintained at 37oC, 5% CO2 in DMEM, with 10% FCS, 1% Penicillin/streptomycin, 1% glutamine and 1% sodium pyruvate added.

A549-RNAi cell line production

A549 were stably transfected with GFP-IRES-shRNAmir constructs purchased from Open Biosystems, UK, to knockdown RASSF8 (RHS3979-98827810 pLKO.1), or a nonsense mRNA sequence (Non-Silencing Control) (pLKO.1) using Fugene HD (ROCHE) according to the manufacturers instructions and maintained in puromycin.

H1792 siRNA transfection:

H1792 cells were transiently transfected with siRNA oligos targeting RASSF8 (Ambion oligo ID 19402) or a siRNA oligo targetting luciferase (MWG) or a non-silencing control sequence (S103650325, QIAGEN, UK) using INTERFERin reagent (Autogen Bioclear) according to manufacturers instructions.

Antibodies

The antibodies used were as follows; anti-RASSF8 (Abnova H00011228-M01, anti-Tubulin (AbCam, ab18251). β-catenin (AbCam, ab32572), E-cadherin (HECD-1, a kind gift from Neil Hotchin, University of Birmingham), NF-κB-p65 (**), total IκB-α (C-21, SantaCruz Biotechnology, Inc, Heidelberg, Germany), alexa-phalloidin (Sigma). Secondary antibodies were purchased from Jackson Immunoresearch (West Grove, PA, USA). All other reagents were purchased from Sigma.

Immunocytochemistry

A549 or H1792 cells cultured on acid-washed glass coverslips, were fixed with 4% paraformaldehyde in PBS and stained with primary antibodies as specified in the text, then appropriate secondary antibodies as described previously (Turner et al., 2006). Filamentous actin was visualized using phalloidin-Alexa594 (Sigma, MO, USA). For epifluoresence microscopy, cells were visualized using a Leica DMRB microscope equipped with a Hamamatsu ORCA camera, and images were captured and processed using OpenLab software (Improvision). For each immunostaining, the same exposure time was used to capture images. For confocal microscopy cells were visualized using a Zeiss LSM 510 confocal and images were captured and processed using LSM image browser software. All pictures were taken sequentially, with a line average of 4.

Immunohistochemistry

Human adenocarcinoma sections with matched clincial notes were obtained from Stretton Scientific (UK) in accordance with all relevant ethical guidelines. Sections were de-waxed and dehydrated before being subjected to 2 minutes high pressure immersion in hot sodium citrate buffer; pH 6.0) for antigen retrieval. Endogenous peroxidase was blocked using hydrogen peroxide, (3% H2O2 in water and 0.5% H2O2 in Methanol), slides washed and then blocked in TNB buffer. Sections were incubated overnight at 4°C in RASSF8 primary antibodies at 1/166 in1% blocking buffer). Secondary goat-anti-mouse biotinylated antibody (1/1000 in 1% blocking buffer, Amersham Life Sciences) was incubated at room temperature for 1 hour. Visualisation was achieved using tyramide signal amplification (TSA: PerkinElmer Life Sciences) followed by 1mg/ml 3,3' diaminobenzidine tetrahydrochloride (DAB Dako Ltd). Sections were counterstained with Gill's Haematoxylin (BDH, UK) using standard protocols. Sections were photographed using a Nikon digital camera at the magnification stated in the text.

EdU incorporation assay

The EdU Click-it system (from??) was used as per manufacturers instructions to analyse proliferation as a measure of the percentage of cells going through S phase, under different experimental conditions, as specified in the text. The mean and SEM of three separate experiments, performed in triplicate, are shown. At least 1200 cells per experiment were counted, repeated 3 times.

Expression analysis

RASSF8 mRNA expression was investigated using normal human cDNA (pre-normalised Clontech MTC panel I; and additionally colon cDNA from BioChain). Primers were designed to amplify across exons 4 to 6 (5'-TCCATTGAGAAACAGCTGGA-3' and 5'-TGGCACAAATCAAAAAGGAA-3'). These primers are specific for the largest isoform of the RASSF8 gene (NM_007211) encoding a 419aa protein (NP_009142).

Mouse in situ:

In situ hybridization was carried out on E15.5 and adult mouse sections using sense and antisense probes as previously described (Charalambous et al., 2003). The probes for RASSF8 were generated from mouse Rassf8 containing pCR-bluntII-topo vector (image clone: 40105476) using a T7 promoter (sense strand) or SP6 promoter (anti sense)following digestion with EconI or PstI enzymes, respectively. Riboprobes were labeled with digoxigenin using the Roche digoxigenin-nucleotide labeling kit according to the manufacturer's instructions. Hybridization was carried out overnight at 60°C in a humidified chamber. The signals were detected by using alkaline phosphatase (AP) labeled anti-digoxigenin Fab fragments (Roche), 1500mU/mL. The staining reaction for alkaline phosphatase was performed at room temperature in darkness with the AP chromogenic substrate, BM purple (Roche).

Luciferase reporter assay

TOPflash (TCF Reporter) luciferase plasmid (Millipore, UK), FOPflash scrambled vector (Millipore, UK), pGL3 basic empty vector (Promega, UK).

The NF-κB-dependent promoter luciferase reporter vector 3nehGL4.2 was constructed by transferring three synthetic copies of the κB consensus of the immunoglobulin κ-chain promoter sequence from the

original 3enh vector (Arenzana-Seisdedos et al., 1993). The 3 neh κB promoter was amplified using forward primer (5'-TTAAGCTTTTTGCAAAAGCCTAGGCC-3') and reverse primer (5'-ATAGCTAGCAGCAGCCCAGTAGTAGG-3'). The resulting PCR product was ligated into the pGEM T easy cloning vector (Promega) and then cloned into the pGL4.22 luciferase vector (Promega) where the luciferase is tagged with 2 degradation sequences to promote degradation of luciferase, and prevent toxic levels accumulating in the cell. Correct insertion was confirmed by plasmid sequencing.

Cells were transiently transfected with 1µg of either 3nehGL4.2 (p65 reporter), TOPFlash, FOPFlash (scrambled control) or pGL3-basic and 0.1µg pRL TK using Fugene HD (ROCHE) according to the manufacturers instructions. Firefly and renilla luciferase activities were assayed 24 hours post-transfection using the dual-reporter assay kit Stop 'N' Glow (Promega). Firefly luciferase activity was normalised to renilla luciferase activity as a transfection control. Promoter activity is expressed as relative luciferase activity compared to that obtained in pGL3basic or FOPFlash (scrambled) control transfected cells, as appropriate.

Soft agar growth assays

For transient knock-down of RASSF8 H1792 lung cancer cells were plated at 5x104 cells per well of a 6 well plate and treated with siRNA oligo directed against luciferase or against RASSF8 using oligofectamine (Invitrogen). Twenty-four hours later cells were trypsinised and plated at 0.5x105 cells per well in soft agar in a 6 well plate. Cells were cultured at 37oC for two weeks, colonies were photographed and the average number of colonies greater than 100µm was calculated and expressed as fold change compared to luciferase siRNA treated controls. Soft agar growth assay using A549 stable RNAi cells were maintained for 5 weeks at 37oC for 5 weeks, colonies were photographed and the average number of colonies greater than 100µm was calculated expressed as fold change compared to NSC-RNAi treated controls.

Scratch wound healing studies

Cells were plated at confluence onto glass Bottom Culture Dishes (MatTek Corporation, MA, USA) and allowed to recover for 24 hours at 37oC, 5% CO2 in normal culture media. Confluent monolayers were wounded with a sterile pipette tip and culture media replaced cell imaging media (CIM) (10µM HEPES-HBSS pH7.4 with 5% FBS). Cells were imaged immediately and 7 hours post-wounding at the same position using a Nikon TE300 epifluorescence microscope (Amstelveen, The Netherlands). Acquisition and editing software used was Openlab 5.0 (Improvision, Coventry, UK). The extent of wound healing was defined as the remaining wound area over the original wound area. This experiment was performed a minimum of three times, with the mean and SE shown.

SDS PAGE and western blotting

Protein lysates were prepared in 3x Laemmli buffer, separated by SDS-PAGE, and immunoblotted as described elsewhere (Croft and Olson, 2006). All experiments were performed on three separate occasions, with representative blots shown.

In vivo tumor growth analysis.

The tumorigenicity of each cell line was tested by s.c. injection of 107 cells in three 4-wk-old female SCID mice, as described previously (wang f et al 2008). Tumour growth in animals was checked twice a week, if tumour formation was observed, tumours were measured using calipers.

Morpholino antisense knockdown

Xenopus laevis eggs were obtained, fertilised and injected with 20ng morpholino into each cell of a two cell embryo according to Sherwood et al 2008. Morpholino oligonucleotides (MO; Gene Tools, Philomath, OR) sequences were as follows:

standard control MO, 5'-CCTCTTACCTCAGTTACAATTTATA-3'

RASSF8 MO1, 5'-ATCGACCCAAACCTTCAGTTCCATC-3'

RASSF8 MO2, 5'-CATCCCCCCAGCGTCATGATTATTG-3'

For western blotting 10 embryos were snap frozen in dry ice, vortexed in 75ul Tris (15mM, pH7.5) and extracted with an equal volume of 1,1,2 Trichlorotrifluoroethane. For immunofluorescence, embryos were fixed in MEMFA for 1h, rinsed with PBS 3x then treated with 20% sucrose in water for 2h before embedding in 15% fish gelatine/15% sucrose in PBS, for cryosectioning. Sections (10uM) were stained according to Sherwood et al., 2008. To detect proliferating cells the ABCam antibody ab14955 against Histone H3 phospho S10 was used at 1:500. The secondary antibody was goat anti mouse A11004 (Molecular probes) used at 1:600 with additional SYTOX green (Molecular probes S7020) diluted 1:5000.

Statistical analysis

Statistical analysis was performed using Student's T-test or Fisher's exact test.

REFERENCES

Barbie DA, Tamayo P, Boehm JS, Kim SY, Moody SE, Dunn IF, Schinzel AC, Sandy P, Meylan E, Scholl C, Fröhling S, Chan EM, Sos ML, Michel K, Mermel C, Silver SJ, Weir BA, Reiling JH, Sheng Q, Gupta PB, Wadlow RC, Le H, Hoersch S, Wittner BS, Ramaswamy S, Livingston DM, Sabatini DM, Meyerson M, Thomas RK, Lander ES, Mesirov JP, Root DE, Gilliland DG, Jacks T, Hahn WC. Systematic RNA interference reveals that oncogenic KRAS-driven cancers require TBK1. Nature. 2009;462(7269):108-12.

Brembeck FH, Rosário M, Birchmeier W. Balancing cell adhesion and Wnt signaling, the key role of beta-catenin. Curr Opin Genet Dev. 2006;16(1):51-9.

Chen L, Johnson RC, Milgram SL. P-CIP1, a novel protein that interacts with the cytosolic domain of peptidylglycine alpha-amidating monooxygenase, is associated with endosomes. J Biol Chem. 1998;273(50):33524-32.

Charalambous M, Smith FM, Bennett WR, Crew TE, Mackenzie F, Ward A. Disruption of the imprinted Grb10 gene leads to disproportionate overgrowth by an Igf2-independent mechanism. Proc Natl Acad Sci U S A. 2003;100(14):8292-7.

Dallol A, Hesson LB, Matallanas D, Cooper WN, O'Neill E, Maher ER, Kolch W, Latif F. RAN GTPase is a RASSF1A effector involved in controlling microtubule organization. Curr Biol. 2009;19(14):1227-32

Dallol A, Agathanggelou A, Fenton SL, Ahmed-Choudhury J, Hesson L, Vos MD, Clark GJ, Downward J, Maher ER, Latif F. RASSF1A interacts with microtubule-associated proteins and modulates microtubule dynamics. Cancer Res. 2004;64(12):4112-6.

Dallol A, Agathanggelou A, Tommasi S, Pfeifer GP, Maher ER, Latif F. Involvement of the RASSF1A tumor suppressor gene in controlling cell migration. Cancer Res. 2005;65(17):7653-9.

Debeer P, Schoenmakers EF, Twal WO, Argraves WS, De Smet L, Fryns JP, Van De Ven WJ. The fibulin-1 gene (FBLN1) is disrupted in a t(12;22) associated with a complex type of synpolydactyly. J Med Genet. 2002;39(2):98-104.

Dejana E and Rudini N. Adherens junctions. 2008, Curr Biol. 18(23):R1080-2.

Deng J, Miller SA, Wang HY, Xia W, Wen Y, Zhou BP, Li Y, Lin SY, Hung MC. beta-catenin interacts with and inhibits NF-kappa B in human colon and breast cancer. Cancer Cell. 2002;2(4):323-34.

Deng J, Xia W, Miller SA, Wen Y, Wang HY, Hung MC. Crossregulation of NF-kappaB by the APC/GSK-3beta/beta-catenin pathway. Mol Carcinog. 2004;39(3):139-46.

Downward J. Cancer: A tumour gene's fatal flaws. Nature. 2009;462(7269):44-5.

Falvella FS, Manenti G, Spinola M, Pignatiello C, Conti B, Pastorino U, Dragani TA. Identification of RASSF8 as a candidate lung tumor suppressor gene. Oncogene. 2006;25(28):3934-8

Gordon MD, Nusse R. Wnt signaling: multiple pathways, multiple receptors, and multiple transcription factors. J Biol Chem. 2006;281(32):22429-33

Katagiri K, Maeda A, Shimonaka M, Kinashi T. RAPL, a Rap1-binding molecule that mediates Rap1-induced adhesion through spatial regulation of LFA-1. Nat Immunol. 2003;4(8):741-8.

MacDonald BT, Tamai K, He X. Wnt/beta-catenin signaling: components, mechanisms, and diseases. Dev Cell. 2009;17(1):9-26.

Meylan E, Dooley AL, Feldser DM, Shen L, Turk E, Ouyang C, Jacks T. Requirement for NF-kappaB signalling in a mouse model of lung adenocarcinoma. Nature. 2009;462(7269):104-7. Epub 2009 Oct 21.

Karin M, Greten FR. NF-kappaB: linking inflammation and immunity to cancer development and progression. Nat Rev Immunol. 2005;5(10):749-59.

Hayden MS, Ghosh S. Shared principles in NF-kappaB signaling. Cell. 2008;132(3):344-62.

Hesson LB, Dunwell TL, Cooper WN, Catchpoole D, Brini AT, Chiaramonte R, Griffiths M, Chalmers AD, Maher ER, Latif F. The novel RASSF6 and RASSF10 candidate tumour suppressor genes are frequently epigenetically inactivated in childhood leukaemias. Mol Cancer. 2009;8:42.

Hesson LB, Cooper WN, Latif F. The role of RASSF1A methylation in cancer. Dis Markers. 2007;23(1-2):73-87.

Hesson LB, Cooper WN, Latif F. Evaluation of the 3p21.3 tumour-suppressor gene cluster. Oncogene. 2007;26(52):7283-301.

Rodriguez-Viciana P, Sabatier C, McCormick F. Signaling specificity by Ras family GTPases is determined by the full spectrum of effectors they regulate. Mol Cell Biol. 2004;24(11):4943-54.

Richter AM, Pfeifer GP, Dammann RH. The RASSF proteins in cancer; from epigenetic silencing to functional characterization. Biochim Biophys Acta. 2009;1796(2):114-28.

Scheel H and Hofmann K (2003). A novel interaction motif, SARAH, connects three classes of tumor suppressor. Curr. Biol. 13: R899–R900.

Sherwood V, Recino A, Jeffries A, Ward A, Chalmers AD. (2009). The N-terminal RASSF family: A new group of Ras association domain containing proteins, with emerging links to cancer formation. Biochem J. in press.

Sherwood V, Manbodh R, Sheppard C, Chalmers AD. RASSF7 is a member of a new family of RAS association domain-containing proteins and is required for completing mitosis. Mol Biol Cell. 2008;19(4):1772-82

Solanas G, Porta-de-la-Riva M, Agustí C, Casagolda D, Sánchez-Aguilera F, Larriba MJ, Pons F, Peiró S, Escrivà M, Muñoz A, Duñach M, de Herreros AG, Baulida J. E-cadherin controls beta-catenin and NF-kappaB transcriptional activity in mesenchymal gene expression. J Cell Sci. 2008;121(Pt 13):2224-34.

Vos MD, Martinez A, Elam C, Dallol A, Taylor BJ, Latif F, Clark GJ. A role for the RASSF1A tumor suppressor in the regulation of tubulin polymerization and genomic stability. Cancer Res. 2004;64(12):4244-50.

Wang F, Grigorieva EV, Li J, Senchenko VN, Pavlova TV, Anedchenko EA, Kudryavtseva AV, Tsimanis A, Angeloni D, Lerman MI, Kashuba VI, Klein G, Zabarovsky ER. HYAL1 and HYAL2 inhibit tumour growth in vivo but not in vitro.PLoS One. 2008;3(8):e3031.

Yeatman TJ. A renaissance for SRC. Nat Rev Cancer. 2004;4(6):470-80.
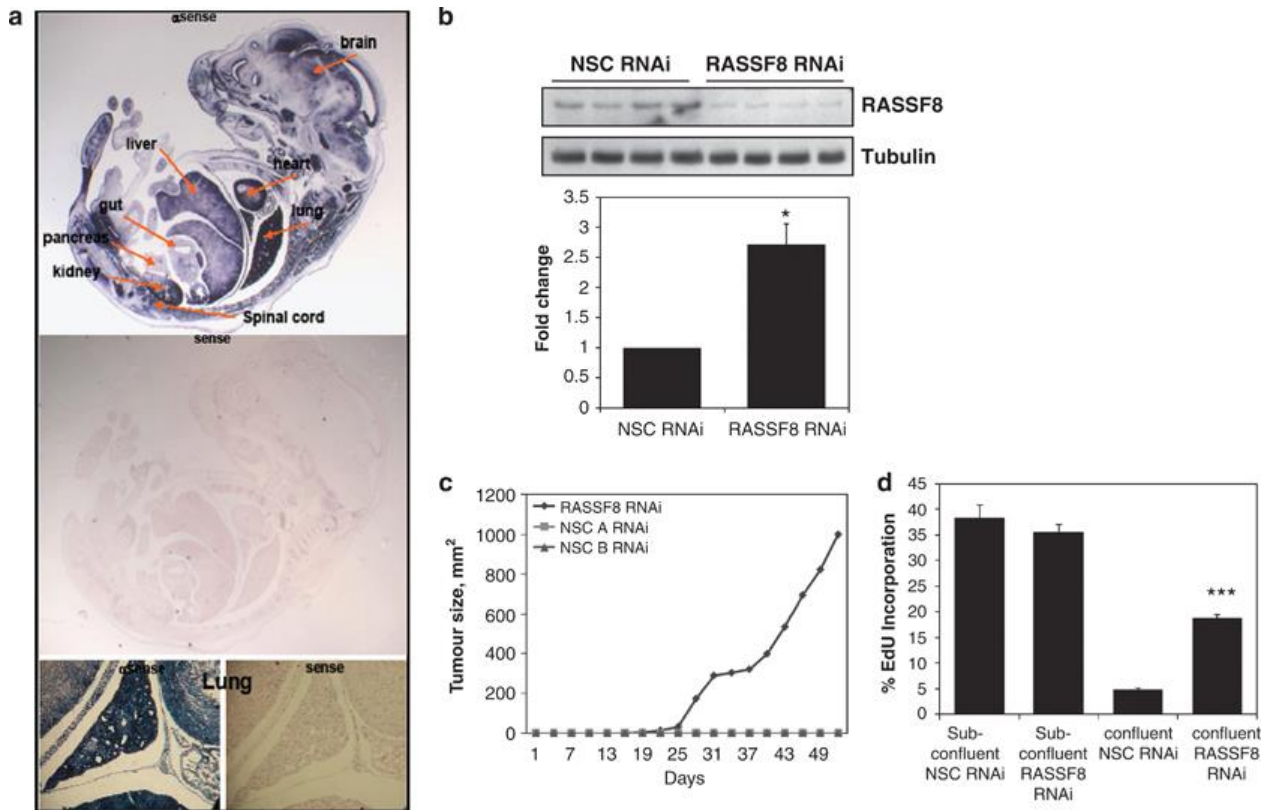
FIGURE 1

RASSF8 mRNA expression and tumor suppression. (A) In situ hybridization to assess RASSF8 RNA expression and localisation in E15.5 embryonic mouse demonstrated Rassf8 mRNA expression in several major organs, including the lung. (B) A549-RASSF8-RNAi, and A549-NSC cell lysates were subjected to Western blotting to analyse RASSF8 expression. RASSF8 expression is knocked down in A549-RASSF8-RNAi lysates compared to NSC controls. Tubulin expression was also assessed as a loading control. (C) A549 RNAi cells were cultured in soft agar for 5 weeks to assess anchorage independent cell growth. The total number of colonies over 100µm across were counted. This experiment was repeated on three separate occasions, mean and SEM are shown as fold change compared to A549 NSC-RNAi cells. * P=<0.05. (D) Tumourigenicity of A549-RASSF8-RNAi and A549-NSC-RNAi control cells was assayed by subcutaneous injection into SCID mice. Animals were maintained according to institutional guidelines. (E) % EdU incorporation for sub-confluent and confluent A549 cells with RASSF8 RNAi or control (NSC) knockdown cells. In confluent cells RASSF8 RNAi vs NSC RNAi, *** P=<0.001. No difference was seen in sub-confluent cells.
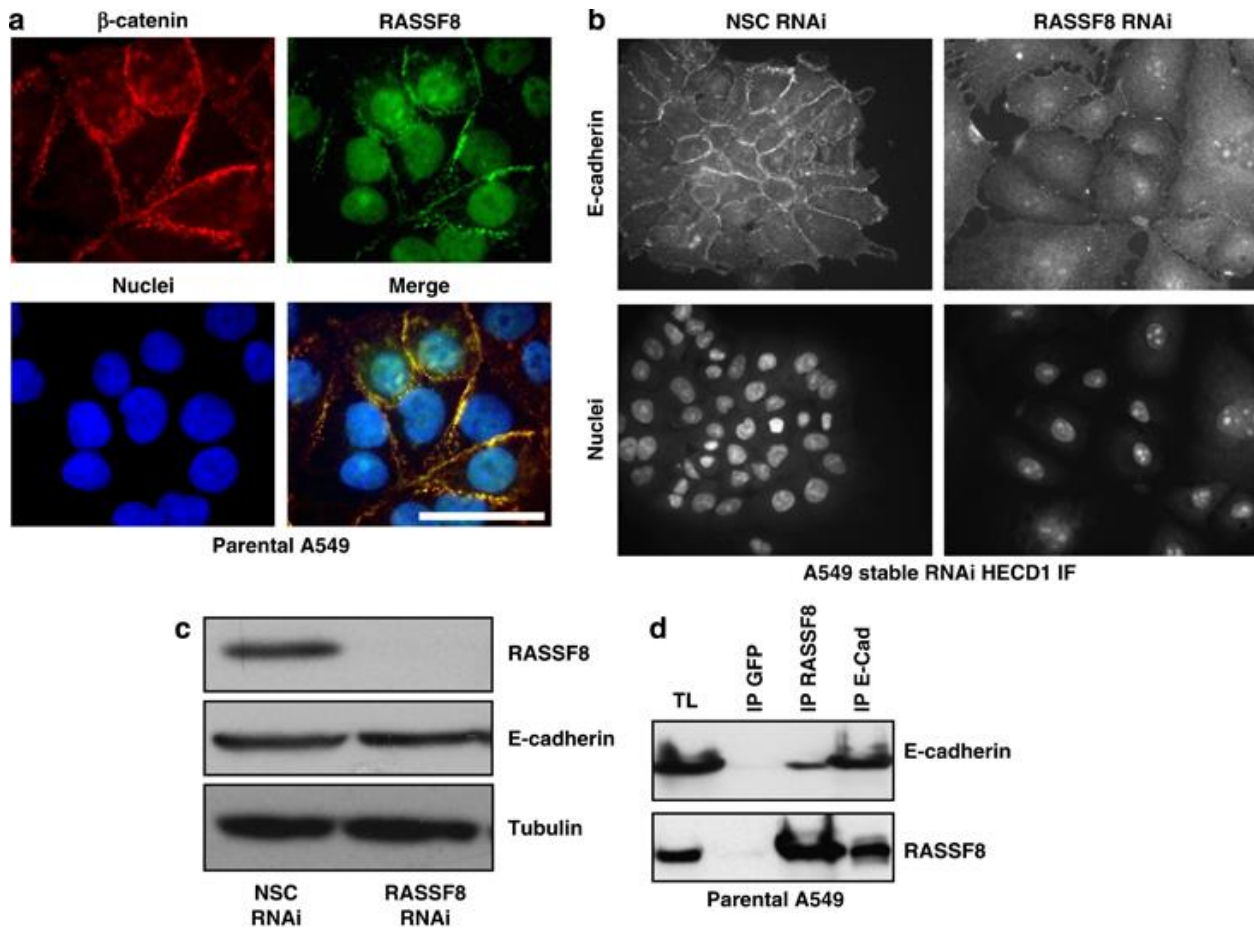
FIGURE 2

Endogenous RASSF8 cellular localization. (A) In order to analyse endogenous RASSF8 localization, parental A549 cells were fixed, stained with RASSF8 and β-catenin antibodies and a nuclear stain, then subjected to confocal microscopy. Endogenous RASSF8 is found in the nucleus and cytoplasm, but is also localised to cell-cell junctions, where it colocalises with β-catenin at adherens junctions. (B) A549-RNAi cells were subjected to epifluorescence immunostaining for E-cadherin. A549-NSC cells grow in well organised colonies, with E-cadherin localised to cell-cell junctions. Following RASSF8 depletion, E-cadherin is lost from cell junctions and cells grow in a more dispersed manner. Insert scale bars!! (C) A549-RASSF8-RNAi, and A549-NSC cell lysates were subjected to Western blotting. No significant changes in E-caderin expression were observed. Tubulin expression was also assessed as a loading control. Blot is representative of 4 separate experiments. (D) A549-RNAi cells were subjected to confocol immunostaining for β-catenin. In A549-NSC cells β–catenin is localized to adherens junctions at the cell periphery. Following RASSF8 depletion, β–catenin is lost from cell junctions and is relocalized to nuclear and peri-nuclear regions in the cell. (E) A549-RASSF8-RNAi, and A549-NSC cell lysates were subjected to Western blotting. No significant changes in ⊠-catenin expression were observed. Tubulin expression was also assessed as a loading control. Blot is representative of 4 separate experiments. (F) The activity of a β-catenin/TCF-dependent promoter (TOP) was determined in A549 RNAi cells by luciferase assay. A549 RNAi cells were transiently transfected with 1 µg TOPFlash (TCF/LEF activity reporter construct) and 0.1 µg of pRL-TK (Renilla luciferase transfection control), cultured for 24h, lysed, and luciferase activity was analyzed. Data shown are the mean and SEM from three separate experiments, expressed as fold change compared to A549-NSC-RNAi cells. P=<0.01. Scale bar represents 10µ meter in all immunofluorescence images.
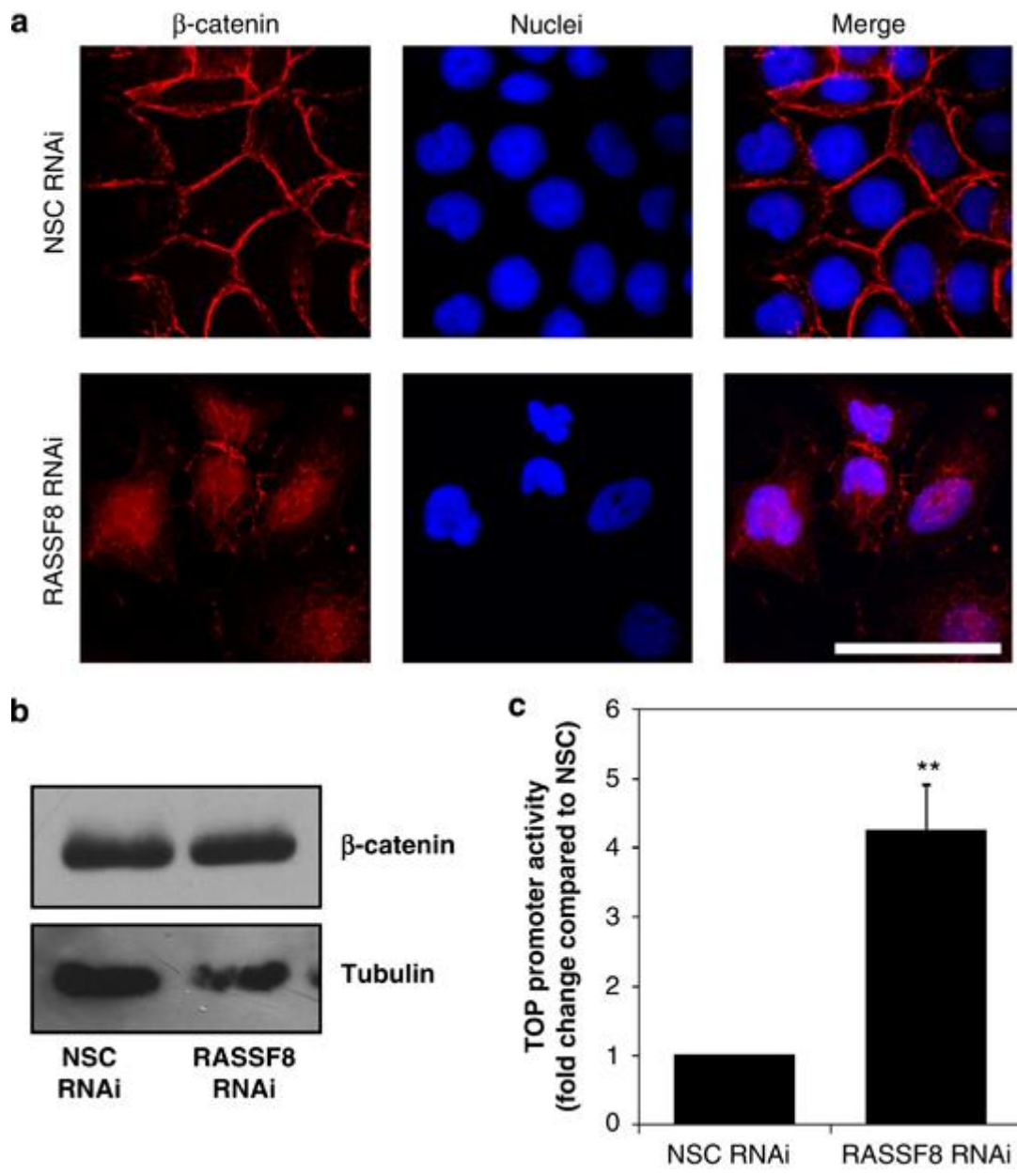
FIGURE 3

RASSF8 depletion results in p65 relocalization. (A) A549 parental cells were fixed, stained using β-catenin and p65 antibodies and examined by confocal microscopy. p65 is localized to the cell periphery, co-localising with β–catenin at adherens junctions. (B) A549-RNAi cells were subjected to confocol immunostaining for p65. In A549-NSC cells p65 is localized to adherens junctions at the cell periphery. Following RASSF8 depletion, p65 is lost from cell junctions and is relocalized to nuclear and peri-nuclear regions in the cell. (C) The activity of a NF-κB-dependent promoter was determined in A549 RNAi cells by luciferase assay. A549 RNAi cells were transiently transfected with 1 μg 3nehGL4.2 (p65 -dependent promoter activity reporter construct) and 0.1 μg of pRL-TK (Renilla Luciferase transfection control), cultured for 24h, lysed, and luciferase activity was analyzed. A small but significant 1.6 fold increase in p65-dependent promoter activity was observed following FASSF8 knockdown. Data shown are the mean and SEM from three separate experiments, expressed as fold change compared to A549-NSC-RNAi cells. P=<0.01 (D) A549-RNAi cellular levels of the p65 regulator IκB-α were analysed by immunoblotting. Following RASSF8 knockdown, IkB- α levels were significantly decreased compared to NSC control cell lysates. Tubulin expression was also assessed as a loading control. This experiment was repeated on three separate occasions, with a representative blot shown. Scale bar represents 10μ meter in all immunofluorescence images.
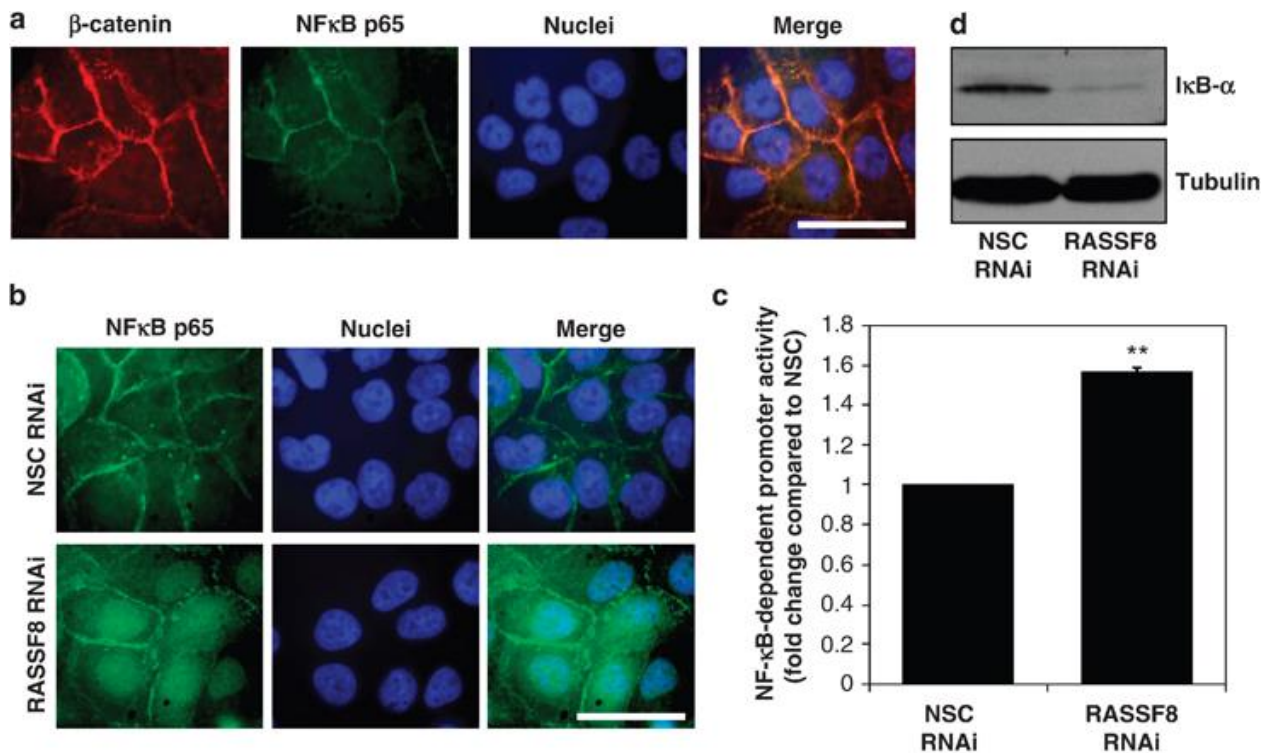
FIGURE 4

RASSF8 depletion results in p65 relocalization. (**a**) A549 parental cells were fixed, stained using β-catenin and p65 antibodies and examined by confocal microscopy. p65 is localized to the cell periphery, co-localizing with β-catenin at adherens junctions (AJs). (**b**) A549-RNAi cells were subjected to confocal immunostaining for p65. In A549-NSC cells p65 is localized to AJs at the cell periphery. Following RASSF8 depletion, p65 is lost from cell junctions and is relocalized to nuclear and perinuclear regions in the cell. (**c**) The activity of a NF-κB-dependent promoter was determined in A549 RNAi cells by luciferase assay. A549 RNAi cells were transiently transfected with 1 μg 3nehGL4.2 (p65 -dependent promoter activity reporter construct) and 0.1 μg of pRL-TK (Renilla Luciferase transfection control), cultured for 24 h, lysed and luciferase activity was analyzed. A significant increase in p65-dependent promoter activity was observed following RASSF8 knockdown. Data shown are the mean and s.e.m. from three separate experiments, expressed as fold change compared to A549-NSC-RNAi cells. **$P<0.01$. (**d**) A549-RNAi cellular levels of the p65 regulator IκB-α were analyzed by immunoblotting. Following RASSF8 knockdown, IκB-α levels were significantly decreased compared to NSC control cell lysates. Tubulin expression was also assessed as a loading control. This experiment was repeated on three separate occasions, with representative blots shown. Scale bar represents 10 μm in all immunofluorescence images.
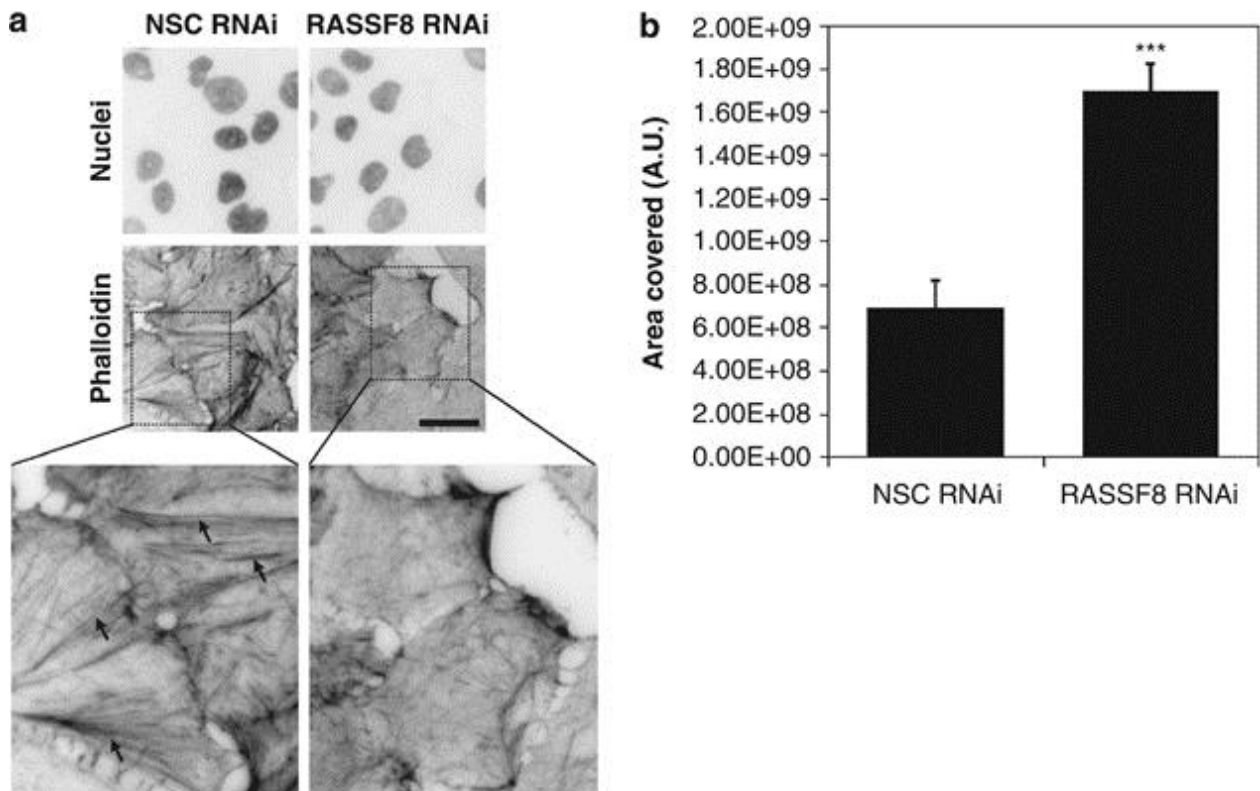
FIGURE 5

RASSF8 role in cell migration. (**a**) A549-RNAi cells were subjected to epifluorescence immunostaining with alexa-phalloidin to visualize the actin cytoskeleton. Images were inverted for clarity. A549-NSC cells have an organized actin cytoskeleton, with actin bundles and stress fibers clearly visible (black arrows). Following RASSF8 depletion, the actin cytoskeleton appears disorganized, with few stress fibers seen. (**b**) RASSF8 role in migration was assessed by scratch wound healing assay. Confluent monolayers of mitotically inactivated A549-NSC and A549-RASSF8 RNAi cells were scratched with a pipette tip and the resulting migration into the 'wound' was assessed. RASSF8 depletion resulted in significantly increased migration compared to NSC-RNAi control cells. ***$P<0.001$.